博士論文

論文題目 The role of CaMKII-Tiam1 complex on learning and memory

（CaMKII-Tiam1複合体の記憶・学習における役割）

氏　　名　　小島　寛人

Contents

Abstract 3

Introduction 4

Material and methods 6

Animal care 6

Reagents and plasmid constructs 6

Antibodies 7

Genotyping 8

Immunohistochemistry 8

Golgi-Cox staining 9

Immunoblot analysis, immunoprecipitation and Pak1 CRIB pull-down assay 9

Hippocampal slice culture and gene transfection 10

Two-photon microscopy imaging and induction of sLTP in single spines 10

Novel object recognition test (NORT) 11

Neuromuscular strength 12

Open field test 12

Rotarod test 13

Hot plate test 13

Y-maze test 13

Light/dark transition test 14

Elevated plus-maze test 14

Porsolt forced swim test 15

Tail suspension test 15

Startle response/prepulse inhibition tests 15

Results 17
Generation of *tiam1* KI mice 17
Spine morphology in *tiam1* KI mice brains 19
The role of CaMKII-Tiam1 interaction in structural plasticity 19
CaMKII-Tiam1 interaction is required for long-lasting memory 20
Behavioral phenotypes of *tiam1* KI mice brains 20
Discussions 23
The role of the CaMKII-Tiam1 complex on learning and memory 23
The physiological meaning of dendritic spine morphology 23
The role of downstream molecules of Tiam1 24
The role of CaMKII-Tiam1-Rac1 signal for learning and memory 25
Figures 26
References 44
Acknowledgment 50

Abstract

In the mammalian central nervous system, excitatory synapses are formed on tiny cellular protrusions called dendritic spines. The structure of the dendritic spines is modified by input activity. A stimulation inducing long-term potentiation (LTP) of synaptic transmission induces a persistent expansion of dendritic spines, a phenomenon recognized as structural LTP (sLTP). The actin cytoskeleton plays an essential role in this process. We previously proposed that the persistent interaction (30 min~) between CaMKII and Tiam1, an activator of Rac1 small G-protein, is a critical mediator of actin regulation. Interestingly, the formation of the complex locks CaMKII into an active conformation, which in turn maintains the activity of Tiam1 through phosphorylation. This makes Rac1 activity persist in the stimulated spine. Therefore, the CaMKII-Tiam1 complex plays a pivotal role in sLTP. To understand the significance of the CaMKII-Tiam1 complex *in vivo*, we generated Tiam1 mutant knock-in mice (*tiam1* KI) in which critical residues for CaMKII binding were mutated into alanines. The *tiam1* KI mice showed similar synaptic protein expression compared to wild type (WT) littermates. Rac1 activity was reduced compared with WT littermates even though the activity of another small GTPase Cdc42 was intact. Although gross appearances of brain structure, histology, as well as spine density were normal in *tiam1* KI mice, the KI mice had shorter spine length and head width. Glutamate-uncaging induced sLTP was abolished in hippocampal CA1 neurons from *tiam1* KI. Moreover, *tiam1* KI mice showed a decreased object recognition memory 7 days after training while the other behavioral tests were normal. Thus, the CaMKII-Tiam1 interaction is not only crucial for sLTP but also required for memory storage.

Introduction

Memory is stored in our brain as a change in the efficiency of neuronal transmissions (Tsien et al., 1996; Whitlock et al., 2006; Nabavi et al., 2014). For instance, when a high frequency stimulation is applied to the hippocampal Schaffer collateral pathway, long-term potentiation (LTP) of synaptic transmissions is observed. The efficiency of neuronal transmissions is modified by changing the number of the AMPA type glutamate receptors (Lu et al, 2009). At the same time, the structure of dendritic spines is modified, which has been named “Structural Plasticity” (Okamoto et al., 2004; Matsuzaki et al., 2004), which allows more glutamate receptors on the synaptic surface by making space. Filamentous actin (F-actin) is the major cytoskeleton in the dendritic spine. A Förster resonance energy transfer (FRET)-based sensor to detect F-actin and G-actin equilibrium showed the equilibrium shifts to F-actin in enlarged spines during LTP. While the structure of dendritic spines is enlarged in response to LTP stimulation, Ca^{2+}/calmodulin-dependent protein kinase II (CaMKII) is activated by Ca^{2+} influx through NMDA receptors. CaMKII is one of the most abundant proteins in the mammalian brain (~0.7 % of the total brain weight, Erondu et al., 1985) and specifically expresses in excitatory neurons. Due to this abundance, in addition to its function as a kinase, CaMKII is thought to have a structural role in synapses. The β isoform of CaMKII binds and bundles F-actin thereby maintaining the spine structure (Okamoto et al., 2007; Kim et al., 2015). CaMKII is transiently activated (~15 sec) during LTP as revealed by a CaMKII FRET sensor Camuiα (Lee et al., 2009). In contrast, actin remodeling lasts more than 30 min. Consistent with this, the activation of Rac1, a regulator of actin cytoskeleton downstream to CaMKII, persists more than 30 min during LTP (Hedrick et al., 2016).

Therefore, there must be a mechanism that converts transient CaMKII to persistent Rac1 signaling.

We previously found that activated CaMKII interacts with Tiam1, a Rac1 specific guanine nucleotide exchange factor (Rac-GEF), in stimulated spines. The interaction is mediated by a “pseudo-autoinhibitory” domain of Tiam1 and a binding pocket “T-site” on CaMKII, normally occupied by the autoinhibitory domain of the kinase. Tiam1 binding interrupts the autoinhibition of the kinase and induces a persistent activation, which, in turn, causes a persistent phosphorylation of Tiam1 and therefore an activation of Rac1 and downstream actin regulators. Based on this observation, we proposed the concept of a “reciprocally activating kinase-effector complex” (RAKEC). However, how this RAKEC-mediated regulation is related to sLTP as well as learning and memory in intact animals is not fully known. In our previous research, we narrowed down the CaMKII binding domain (CBD) on Tiam1 to 1540-1591 amino acid residue which is downstream to the DH-PH domain with Rac-GEF activity (aa 1044–1397) (Saneyoshi et al., under revision; Tolias et al., 2005; Worthylake et al., 2000). Alanine mutations in 1552-1554 residue caused disruption of CaMKII-Tiam1 interaction *in vitro* (Saneyoshi, under revision). Thus, this mutant could be a useful tool to understand roles of CaMKII-Tiam1 *in vivo* such as learning and memory.

In this thesis work, we generated *tiam1* KI mice harboring the alanine mutations in CBD to understand the roles of the CaMKII-Tiam1 complex in brain function. The *tiam1* KI mice were born at the expected Mendelian inheritance ratio and showed no grossly apparent abnormality. However, the spine morphology was abnormal and sLTP was abolished in hippocampal CA1 neurons of *tiam1* KI. In addition, object recognition memory was impaired in the *tiam1* KI mice 7 days after training. We

concluded, that CaMKII-Tiam1 interaction is required for sLTP and memory storage.

Material and methods

Animal care

Animal experiments were performed with the approval of the Animal Care and Use Committee of Kyoto University Graduate School of Medicine and the Animal Experiment Ethics Committee at the University of Tokyo and according to the University of Tokyo guidelines for the care and use of laboratory animals. Male 8- to 12-week-old C57BL/6J mice were housed under conditions of controlled temperature and humidity, maintained on a 12:12-h light/dark cycle with the lights on from 7:00 a.m. to 7:00 p.m., and had access to food and water *ad libitum*. Behavioral testing was performed between 9:00 a.m. and 6:00 p.m.

Reagents and plasmid constructs

TBS (Tris-buffered saline): 137 mM NaCl, 2.7 mM KCl, 25 mM Tris-HCl (pH 7.5)

TBS-T: TBS with 0.05% (v/v) Tween 20. 0.1% n-dodecyl-β-D-maltopyranoside (DDM, Dojindo): 150 mM NaCl, 50 mM TrisHCl (pH 8.5), 10% glycerol, 10 mM glycerophosphate, 1 mM Na_3VO_4, 10 mM $MgCl_2$, and 0.2 mM $CaCl_2$. Complete protease inhibitor cocktail (Roche) and phosphatase inhibitor cocktail (Nacalai tesque) were added before use. BOS lysis buffer: 1% (w/v) NP40, 50 mM Tris-HCl (pH 7.4), 200 mM NaCl, 10% (v/v) Glycerol, 0.5 mM β-Glycerophosphate, 10 mM $MgCl_2$, and 0.2 mM $CaCl_2$. Complete protease inhibitor cocktail (Roche) and phosphatase inhibitor cocktail (Nacalai tesque) were added before use. IP Wash buffer: 20 mM Tris-HCl (pH 8.0), 150 mM NaCl, 0.1% (w/v)

DDM, 5% (v/v) glycerol. GST Wash buffer: TBS, 1 M NaCl. 2x SDS-PAGE sample buffer: 62.5 mM Tris-HCl (pH 6.8), 10% glycerol, 2% SDS, 5% 2-mercaptoethanol, 0.005% Bromophenol Blue. SDS running buffer: 25 mM Tris, 192 mM glycerol, 0.1% (w/v) SDS. SDS transfer buffer: 25 mM Tris, 192 mM glycerol, 20% (v/v) methanol. Primary antibody dilution buffer: TBS-T, 1% (w/v) BSA, 0.02% (w/v) NaN_3. Primary antibodies were diluted at 1:1000 ratio. Secondary antibody dilution buffer: TBS-T, 5% (w/v) skim milk. Secondary antibodies were diluted at 1:5000 ratio. Mouse Tiam1 was cloned from mouse brain cDNA library (Saneyoshi et al., 2008). The plasmids encoding myc-CaMKII and FLAG-TIAM1 were generated with standard method. The CaMKII-Tiam1 binding dead mutant was generated by site-directed mutagenesis using QuikChange Multi Site-Directed Mutagenesis Kit (Agilent Technologies).

Antibodies

For immunostaining, immunoprecipitation and western blot analysis, the following antibodies were used: β-actin (1:1000, Santa Cruz Biotechnology), β-PIX (1:1000, Cellsignaling), CaMKII (1:1000, BD Bioscience), Cofilin1 (1:1000, Cell signaling), GluA1 (1:1000, abcam), GluN2B (1:1000, milipore), Homer 1b/c (1:1000, Santa Cruz Biotechnology), Kalirin-7 (1:1000, Millipore), Limk1 (1:1000, BD BIoscience), NeuN (1:100, abcam), Pak1 (1:1000, Cell signaling), PSD95 (1:1000, Santa Cruz Biotechnology), Rac1 (1:1000, BD BIoscience), Tiam1 (R&D Systems for immunoprecipitation, 1:1000, Santa Cruz Biotechnology for Westarn).

Genotyping

For DNA extraction, mouse tail biopsy specimens were incubated for 10 min at 95-100 °C with 120 µl of 50 mM NaOH. Then the solubilized tissue was neutralized with 80 µl of 1 M Tris-HCl (pH 8.0) and centrifuged to remove debris. The supernatant was used as a template for PCR. PCR condition was as follows: 94 ºC for 2 min, 40 x [94 ºC for 20 s, 60 ºC for 30 s, 72 ºC for 30 s], 72 ºC for 2 min. The following primers were used for genotyping, Fw primer; 5'-CTGCCCCAAGCAAGTCTCTT-3', Rv primer for mutant; 5'-GTGCCGCTTGCGCCG-3', Rv primer for wt; 5'-AGGGCCGCTTGCTTCTTG-3', designed by primer BLAST. The primer for the sequencing of Tiam1 genome; 5'-GTACGAGGAGCAGGATGACA-3'.

Immunohistochemistry

The mice were transcardially perfused with 4 % (w/v) paraformaldehyde (PFA)/PBS. The brains were then removed and submerged in 4 % PFA, at 4 °C, for 1 day. The medium was replaced by PBS and incubated, at 4 °C, for 1 day. Whole brains were sliced at 100 µm thickness by a vibratome. Then, the sections were incubated with primary antibodies (1:100) diluted by TNB buffer +0.5 % Triton-X100 at 4 °C, for 1 day. After washing with TBS three times, the sections were incubated with Hoechst (1:1000, Calbiochem), Phalloidin Alexa Fluor 594 (1:200, thermofisher) secondary antibodies (1:500, anti-mouse Alexa Fluor 488 or anti-rabbit Alexa Fluor 488, thermofisher) diluted by TNB buffer +0.5 % Triton-X100 at 4 °C, for 1 hour. After washing with TBS three times, the brains were mounted on cover slips with a drop of

mounting media (VECTASHIELD, Vector laboratories). The TNB buffer was composed of 0.1 M Tris-HCl (pH 7.5), 0.15 M NaCl, 0.5 % blocking reagents (w/v). Images were taken by BZ-X700-All-in-One Fluorescence Microscope (KEYENCE).

Golgi-Cox staining

Freshly dissected mouse brains were submerged in Golgi-Cox solution containing 5% (w/v) potassium dichromate and an equivalent 5% (w/v) mercury (II) chloride, adding an equivalent 5% (w/v) potassium chromate. The brains were incubated in a dark room at room temperature for 2 days. The medium was then changed to fresh Golgi-Cox solution and the brains further incubated in a dark room at room temperature for 5 days. The medium was finally replaced by 30% sucrose solution and the brains incubated at room temperature for 2 days. The whole brains were sliced into 200 μm thickness by vibratome. Then, the sections were placed into a 15 ml tube filled with dH_2O and washed twice. The precipitation of metallic mercury was performed with 28% ammonia water for 30 min. The sections were dehydrated with a graded alcohol series (50, 70, 80, 90, and 100%). After cleaning three times with xylene, the sections were left in the solution consisting of 1:1:1 mixture of xylene, chloroform, and ethanol for 2 h in darkness. Each slice was taken out carefully and mounted on slides with Entellan New.

Immunoblot analysis, immunoprecipitation and Pak1 CRIB pull-down assay

Mouse forebrains were homogenized with 9 volumes of the BOS lysis buffer for pull-down assay or 0.1% DDM for immunoprecipitation. Then the tissue lysates were centrifuged at 100,000 g for 1 hour and the supernatant was obtained. Each one

milliliter of the supernatant was subjected to GST-pull down assay with 50 µg of GST-PAK1-CRIB plus 25 µl of glutathione agarose (GST-accept, Nacalai tesque) or immunoprecipitation with 50 µg of protein G agarose plus 5ug of anti TIAM1 antibody or IgG. Then the lysate was rotated at 4°C for 3 hours. After washing with the lysis buffer 3 times, bound proteins were eluted with 100 µl of 2 x sample buffer. Western blotting was performed as previously described (Saneyoshi et al., 2008) and the signal was quantified using the Image-J software.

Hippocampal slice culture and gene transfection

Hippocampal organotypic slice cultures were prepared from postnatal day 6-7 rats or mice as previously described (Okamoto et al., 2004). Slices were cultured at 35ºC on interface membranes (Millipore) and fed with MEM containing 20% horse serum, 27 mM D-glucose, 6 mM $NaHCO_3$, 2 mM $CaCl_2$, 2 mM $MgSO_4$, 30 mM HEPES, 0.01% ascorbic acid and 1 µg/ml insulin. The pH was adjusted to 7.3 and osmolarity to 300-320 mOsm. Slices were transfected after DIV 5-7 with a plasmid encoding GFP by ballistic method (Gene-gun, Biorad).

Two-photon microscopy imaging and induction of sLTP in single spines

Imaging was carried out with a two-photon microscope (Olympus) with two Ti:sapphire lasers (Sprectra-Physics) in apical dendrites of CA1 pyramidal neurons (Bosch et al., 2014). sLTP was induced on small mushroom spines by uncaging MNI-glutamate with 2 ms laser pulses (5 mW, 720 nm) repeated at 1 Hz for 0.5 min in Mg-free solution (Matsuzaki et al., 2004). GFP was excited at 910 nm. Slices were maintained at room temperature (25-27°C) in a continuous perfusion of

artificial cerebrospinal fluid (ACSF) containing 119 mM NaCl, 2.5 mM KCl, 3 mM $CaCl_2$, 26.2 mM $NaHCO_3$, 1 mM NaH_2PO_4 and 11 mM glucose, 1 μM tetrodotoxin, 50 μM picrotoxin and 2.5 mM 4-methoxy-7-nitroindolinyl (MNI)-L-glutamate (Tocris, Bristol, UK) equilibrated with 5% CO_2/95% O_2. GFP intensity in each spine was calculated using ImageJ.

Novel object recognition test (NORT)

The NORT consisted of 3 sessions: habituation, training, and memory test. Before each session, the mice cages were moved to a behavior test room and left for 15 min. After being handled for a week, the habituation session was performed. The mice were placed near a wall of the open field arena (50×50×50 cm) and allowed to explore for 15 min. The mice were then returned to its home cage. One day after habituation, the training session was performed. In the training session, two identical objects were placed near the corners of one wall in the arena (5 cm from each adjacent wall). The mice were placed near the wall opposite from the objects and allowed to explore for 15 min. The mice were then returned to its home cage. For the test session, the mice were divided into two separate groups.1 day after the training session for the first group, or 7 days for the second group of mice, a test session was performed. On the day of the test session, two objects were placed in the same position as in the training session. One object was replaced by a new object (novel). The mice were placed near the opposite side wall of the objects and allowed to explore for 5 min. The mice were then returned to its home cage. Explorative behavior was defined as sniffing or touching the object with nose and/or forepaws. Sitting on the object was not considered as exploration. The memory score from NORT was calculated as a discrimination ratio

for each mouse with the following formula: (T2-T1)/(T1+T2) [T1 = time spent exploring the familiar object, T2 = time spent exploring the novel object]. Between trials, the objects and the field were wiped with 70% ethanol solution.

Neuromuscular strength

The neuromuscular strength was measured with the grip strength test and wire hang test (Yamasaki et al., 2008). A grip strength meter (O'Hara & Co., Tokyo, Japan) was used to assess forelimb grip strength. The mice were lifted and held by their tail so that their forepaws could grasp a wire grid. The mice were then gently pulled backward by the tail with their posture parallel to the surface of the table until they released the grid. The peak force applied by the forelimbs of the mouse was recorded in Newtons (N). Each mouse was tested three times, and the greatest value measured was used for statistical analysis. In the wire hang test, the mouse was placed on a wire mesh that was then inverted and waved gently, so that the mouse gripped the wire. Latency to fall was recorded, with a 60 s cut-off time.

Open field test

Locomotor activity was measured using an open field test (Holmes, 2001; Belzung & Griebel, 2001; Yamasaki et al., 2008). Each mouse was placed in the center of the open field apparatus (40 × 40 × 30 cm; Accuscan Instruments, Columbus, OH). Total distance traveled (in cm) and time spent in the center were recorded. Data was collected for 60 min.

Rotarod test

Motor coordination and balance were tested with the rotarod test (Yamasaki et al., 2008). The rotarod test, using an accelerating rotarod (UGO Basile Accelerating Rotarod), was performed by placing the mice on rotating drums (3 cm diameter) and measuring the time each animal was able to maintain its balance on the rod. The speed of the rotarod accelerated from 4 to 40 rpm over a 5 min period.

Hot plate test

The hot plate test was used to evaluate sensitivity to a painful stimulus (O'Callaghan & Holtzman, 1975; Yamasaki et al., 2008). The mice were placed on a 55°C hot plate (Columbus Instruments), and latency to the first hind-paw response was recorded. The hind-paw response was defined as either a paw shake or a paw lick.

Y-maze test

The Y-maze was performed to check spatial working memory and schizophrenia-like behavior (Belforte et al., 2010; Le Pen et al., 2006; Yamasaki et al, 2008). A Y-shaped maze with three white, opaque plastic arms at a 120° angle from each other was used. After introduction to the center of the maze, the mouse was allowed to freely explore the three arms for 5 min. The number of arm entries was recorded in order to calculate the percentage of alternation. An entry occurred when all four limbs were within the arm. The percentage of alternation was calculated by the following formula: N1/(N2-2) [N1 = The number of entry sequences into arms other than the one which the mice had entered just before, for at least three times consecutively, N2 = The total number of entries into any arm].

Light/dark transition test

The light/dark transition test was performed to check anxiety-like behavior (Cryan & Holmes, 2005; Yamasaki et al., 2008). The apparatus used for the light/dark transition test consisted of a cage (21 × 42 × 25 cm) divided into two sections of equal size by a partition containing a door (O'Hara & Co., Tokyo, Japan). One chamber was brightly illuminated (390 lux), whereas the other chamber was dark (2 lux). The mice were placed into the dark side and allowed to move freely between the two chambers with the door open for 10 min. The total number of transitions between chambers, the time spent on each side, the first latency to enter the light side as well as the distance traveled were recorded automatically.

Elevated plus-maze test

The elevated plus-maze test was performed to test anxiety-like behavior (Cryan & Holmes, 2005; Yamasaki et al, 2008). The apparatus (O'Hara & Co., Tokyo, Japan) consisted of two open arms (25 × 5 cm) and two enclosed arms of the same size, with 15-cm high transparent walls. The arms and central square were made of white plastic plates and were elevated to a height of 55 cm above the floor. To minimize the likelihood of animals falling from the apparatus, 3-mm high plastic ledges were provided for the open arms. Arms of the same type were arranged at opposite sides to each other. Each mouse was placed in the central square of the maze (5 × 5 cm), facing one of the closed arms. The mouse's behavior was recorded during a 10-min test period. The number of entries into, and the time spent in open and enclosed arms, were recorded. For data analysis, the following four measures were used: the percentage of

entries into the open arms, the time spent in the open arms (s), the number of total entries, and total distance traveled (cm). Data acquisition and analysis were performed automatically using Image EP software (Yamasaki et al., 2008).

Porsolt forced swim test

The Porsolt forced swim test was performed to test depression-like behavior (Cryan & Holmes, 2005; Yamasaki et al., 2008). The apparatus consisted of four plastic cylinders (20 cm height × 10 cm diameter). The cylinders were filled with water (23°C) up to a height of 7.5 cm. The mice were placed into the cylinders and their behavior recorded over a 10-min test period. Data acquisition and analysis were performed automatically, using Image PS software. The distance traveled was measured by Image OF software (Yamasaki et al., 2008) off-line.

Tail suspension test

The tail suspension test was performed to test depression-like behavior (Cryan & Holmes, 2005; Yamasaki et al., 2008). The mice were suspended 30 cm above the floor in a visually isolated area by adhesive tape placed 1 cm from the tip of the tail, and their behavior was recorded over a 10 min test period. Data acquisition and analysis were performed automatically, using Image TS software (Yamasaki et al., 2008).

Startle response/prepulse inhibition tests

Startle response/prepulse inhibition tests were performed with 9 to 11-week-old male mice to check schizophrenia-like behavior(Yamasaki et al., 2008). A startle reflex

measurement system was used (O'Hara & Co., Tokyo, Japan) to measure startle response and prepulse inhibition. A test session began by placing a mouse in a plastic cylinder where it was left undisturbed for 10 min. White noise (40 ms) was used as the startle stimulus for all trial types. The startle response was recorded for 140 ms (measuring the response every 1 ms) starting with the onset of the prepulse stimulus. The background noise level in each chamber was 70 dB. The peak startle amplitude recorded during the 140 ms sampling window was used as the dependent variable. A test session consisted of six trial types (i.e. two types for startle stimulus only trials, and four types for prepulse inhibition trials). The intensities of the startle stimulus were 90, 100, 110 or 120 dB. The prepulse sound was presented 100 ms before the startle stimulus, and its intensity was 74 or 78 dB. Four combinations of prepulse and startle stimuli were used (70–120, 75–120, 80–120, and 85–120). Six blocks of the six trial types were presented in pseudorandom order such that each trial type was presented once within a block. The average inter-trial interval was 15 s (range: 10–20 s).

Results

Generation of *tiam1* KI mice

To generate *tiam1* KI mice with a deficit of CaMKII-Tiam1 binding, we applied the CRISPR/Cas9 genome editing technology to introduce mutations in the CaMKII binding domain of Tiam1 (1552-1554, LKK-AAA) (Incontro et al., 2014; Shan, 2014) (Fig. 1A). First, we designed 4 sgRNAs targeted against the vicinity of the mutation site with high on-target and low off-target effects using a web tool (https://benchling.com). Each sgRNA was subcloned into pX330 and verified by sequencing (Cong et al., 2013) (Fig. 1B) To check the efficacy of sgRNAs, we co-transfected each of them with pX330 sgRNA construct together with Cas9 and mouse Tiam1 cDNA into HEK293T cells. The expression level of Tiam1 was analyzed by immunoblotting. From among the 4 sgRNAs, we chose #1 because it showed the highest reduction of Tiam1 expression for injection into fertilized eggs (Fig. 1C, 2A). The sgRNA, Cas9 mRNA, Tiam1 1552-1554 AAA oligo DNA were injected into cytoplasm, nuclei or both of the eggs. Then the injected eggs were returned into pregnant mice. We obtained 69 pups from 500 injected eggs, out of which 19 mice showed the heterozygous *tiam1* KI mutation and 4 showed the homozygous *tiam1* KI mutation (Fig. 2B). We then backcrossed the homozygous *tiam1* KI mice with WT C57BL/6 mice twice. The *tiam1* KI mice were born at the expected Mendelian ratio and did not show any abnormality in body weight, gross appearance or behavior. There was also no difference in brain size, weight or the overall morphology, nor the layer structures of the brain between *tiam1* KI and WT (Fig. 4A-G).

We performed immunostaining against Tiam1, which showed a similar expression pattern of Tiam1 among WT and *tiam1* KI mice (Fig. 4C). We then

checked if the CaMKII-Tiam1 interaction was disrupted in *tiam1* KI by co-immunoprecipitation of CaMKII and Tiam1 using anti-Tiam1 antibody from brain tissue. The brain was homogenized with 0.1% DDM lysis buffer supplemented with 0.2 mM $CaCl_2$ to mimic activity dependent interaction in stimulated spines. The brain lysate was then subjected to immunoprecipitation with anti-Tiam1 antibody. Co-immunoprecipitated CaMKII with Tiam1 was significantly lower in *tiam1* KI than in wild-type littermates (Fig. 3A, B), confirming that CaMKII-Tiam1 interaction was impaired in *tiam1* KI mice.

Next, we examined the level of representative synaptic protein expressions in *tiam1* KI mice by western blotting. The *tiam1* KI mice did not show any difference in the level of the postsynaptic AMPA and NMDA type glutamate receptor subunits, the scaffolding proteins PSD-95 and Homer1b/c, signaling molecules CaMKII and LIMK1, or actin cytoskeleton molecules β-actin and cofilin (Fig. 5A, B). Thus, the *tiam1* mutant KI affected neither neuronal development nor synaptic protein expression.

As we have proposed that the CaMKII-Tiam1 complex enables persistent Rac1 activity (Saneyoshi et al., unpublished), we wondered if the Rac1 activity would be affected in *tiam1* KI. To examine the Rac1 activity we used the Pak1 pull-down assay with Cdc42/Rac1 interactive binding (CRIB) domain to concentrate active Rac1 protein (Saneyoshi et al., 2008). As a result, *tiam1* KI mice showed significantly lower Rac1 activity compared to their WT littermates (Fig. 6A, B). The activity of Cdc42 was not significantly different between *tiam1* KI and WT, showing a selectivity of deficiencies. Therefore, we could confirm that our *tiam1* KI mice had a deficit of CaMKII-Tiam1 interaction and Rac1 activity.

Spine morphology in *tiam1* KI mice brains

Because Tiam1 is important for spine morphogenesis (Zhang & Macara, 2006; Tolias et al, 2005, 2007), CaMKII-Tiam1 interaction might play a critical role in spine structure. First, we examined if the density of dendritic spines had an effect by disrupting CaMKII-Tiam1 interaction in CA1 pyramidal neurons. The brain was subjected to Golgi-Cox staining to label neurons sparsely from tissue (Zaqout & Kaindl, 2016; Kang et al., 2017). The density of dendritic spines in the hippocampus CA1 region of *tiam1* KI mice did not show any difference compared with WT (Fig. 7C). In contrast, the spine length and head width in *tiam1* KI mice showed a significant reduction in *tiam1* KI as compared to WT mice (Fig. 7D). Because the spine width is related to the efficiency of synaptic transmission (Matsuzaki et al., 2004; Harvey et al., 2007), the synaptic transmission efficiency might be decreased in *tiam1* KI mice.

The role of CaMKII-Tiam1 interaction in structural plasticity

We then wondered whether CaMKII-Tiam1 interaction plays a role in plasticity-related spine morphogenesis. We conducted 2-photon glutamate uncaging (2P-GU) to examine if the CaMKII-Tiam1 interaction was required for structural LTP. In WT neurons, the size of dendritic spines was enlarged and maintained for 30 min by uncaging stimulation while not stimulated nearby spines did not show any changes. However, the structure of dendritic spines in *tiam1* KI was not enlarged in response to 2P-GU (Fig. 8B). The average volume change of spines in the transient (1-3 min after stimulation) and sustained phase (21-30 min after stimulation) showed a significant

decrease of volume enlargement after stimulation in KI mice (Fig. 8C). Therefore, we concluded that CaMKII-Tiam1 interaction is necessary for sLTP.

CaMKII-Tiam1 interaction is required for long-lasting memory

Next, we examined the role of CaMKII-Tiam1 on learning and memory. There are few reports on the relationship between the structural change of spines and learning and memory. It is not well understood if sLTP is required for learning and memory. Using *tiam1* KI mice, we could also examine the physiological meaning of sLTP. To examine learning and memory we used the novel object recognition task (NORT). It has been reported that hippocampus and perirhinal cortex are required for object recognition memory in NORT. First, we checked the object recognition memory 1 day after training with one group of mice. The mice were trained and subjected to the test trial (Fig. 9A). The results showed, that the memory of *tiam1* KI mice was marginally lower but no statistically significant compared with WT littermates (Fig. 9B). We then examined the memory score 7 days after training in NORT with the other group of mice. The memory score 7 days after training was significantly decreased in *tiam1* KI mice compared with WT (Fig. 9C). From these results it can be said, that CaMKII-Tiam1 dependent sLTP is not required for the acquisition of object recognition memory but for the maintenance of recognition memory.

Behavioral phenotypes of *tiam1* KI mice brains

Because spine morphology is not only related to learning and memory but also other behavioral phenotypes such as anxiety, depression, autism and schizophrenia, we also conducted behavioral battery tests. Rectal temperature and muscle strength were not significantly different between *tiam1* KI mice and WT (Fig. 10 A-D). Next, we

performed an open field test to check locomotor activity in KI mice. The mice were allowed to move freely in the open field. As an anxiety-like behavior, decreased time spent in the center area of the open field (10 cm apart from the walls) was observed (Holmes, 2001; Belzung & Griebel, 2001). As a result, the open field test showed no difference of total distance in 1 hour and time spent in the center area of the open field between WT and KI mice, which suggests that the KI mice had normal locomotor activity and no anxiety-like phenotype (Fig. 11 A-C). In addition, pain sensitivity and motor learning were evaluated by a hot plate test and a rotarod test respectively. In the hot plate test, the time spent on the hot plate was measured as pain sensitivity. In the rotarod test, the time spent on the rotor rod was measured as motor learning. In both tests, there was no significant difference of each score between WT and KI mice, which suggests that KI mice had normal pain sensitivity and have no disability of motor skills (Fig. 12 A-C). We also performed a Y-maze test to check the working memory in KI mice. The mice were allowed to freely move in the Y-maze and the number of entries into any arm and the total alteration were measured as working memory and schizophrenia-like behavior (Belforte et al., 2010; Le Pen et al., 2006). The results showed no difference in the number of entries into arms and total alteration between WT and KI mice (Fig. 13 A, B). This result suggests that KI mice have neither a deficit of working memory nor schizophrenia-like behavior in the Y-maze test.

We then examined the effect of Tiam1 mutant KI on mental illnesses. Anxiety-like behavior was evaluated by a light/dark transition test and an elevated plus maze test. The mice were allowed to move on an elevated plus maze or in a light box connected with a dark box. In the elevated plus maze test, the increase of latency in the

closed arms and the number of entries into the closed arms were observed as anxiety-like behavior (Cryan & Holmes, 2005). In the light/dark transition test, the increase in the latency to move to the dark room and the number of transitions into the dark room were interpreted as anxiety-like behavior (Cryan & Holmes, 2005). In both tasks, *tiam1* KI mice did not show anxiety-like behavior (Fig. 14 A-D).

In addition, depression-like behavior was evaluated by a Porsolt forced swim test and tail suspension test. In the Porsolt forced swim test, the mice were forced to swim in a plastic cylinder filled with water for 10 min and immobile time was measured as a depression-like behavior (Cryan & Holmes, 2005; Yamasaki et al., 2008). In the tail suspension test, the mice were suspended from 30 cm above the floor for 10 min per day, for two days. The immobile time of every minute was measured as a depression-like behavior (Cryan & Holmes, 2005; Yamasaki et al., 2008). *tiam1* KI mice did not show depression-like behavior (Fig. 15 A-C).

Next, we evaluated the schizophrenia-phenotype in *tiam1* KI mice by a prepulse inhibition test. In the prepulse inhibition test, decreased prepulse inhibition is observed as a schizophrenia-like behavior (Geyer et al., 2001). Interestingly, *tiam1* KI mice showed significantly lower prepulse inhibition, which implicates the involvement of this pathway in the pathogenesis of schizophrenia (Fig. 16 A, B). Figure 16 should be explained in relation with the schizophrenic phenotype.

Discussions

The role of the CaMKII-Tiam1 complex on learning and memory

Our previous research showed that CaMKII-Tiam1 interaction persists for more than 30 min in a spine which underwent sLTP and this interaction is necessary for persistent Rac1 activity. Our current research concludes that CaMKII-Tiam1 interaction is necessary for persistent Rac activity and sLTP. Next, we have another question: how sLTP is related to memory maintenance? First of all, sLTP is thought to enhance the efficiency of synaptic transmission (Matsuzaki et al., 2004; Harvey et al., 2007). Based on this, there are two possible relations between sLTP and memory maintenance. One is that if sLTP is maintained for more than several days, in which case, memory engram cells can be maintained in the brain region in which memory is formed, such as the hippocampus. And also sLTP enables access to these engram cells for a long time and retrieve memory even several days after memory formation. As the second possibility, if sLTP is maintained for less than several days, it becomes possible for memory engram cells to transfer to another brain region such as the retrosplenial cortex (RSC), anterior cingulate cortex (ACC) or/and locus coeruleus (LC) (Xu & Südhof, 2013). In this case, sLTP probably makes memory consolidated in the cortex.

The physiological meaning of dendritic spine morphology

Structural changes of dendritic spines are separated into at least 4 patterns, which are enlargement, shrinkage, formation and disappearance. Especially spine formation is mainly observed after a learning process in *in vivo* mouse brains (Yang et al., 2009; Xu et al., 2009). And newly formed spines tend to make spine clusters depending on each task (Fu et al., 2012; Schmid et al., 2016; Frank et al., 2018). Probably, clustered

spines induce spine enlargement and enhancement of synaptic transmission as well (Harvey et al., 2007; Cichon et al, 2015). From this evidence *in vivo* and *in vitro*, spine formation is required for memory formation and spine enlargement is required for memory maintenance. For spine formation, there might be different mechanisms from spine enlargement. To understand the distinct mechanism, tools to regulate the spine morphology under *in vivo* observation are required.

The role of downstream molecules of Tiam1

While structural plasticity occurs, actin filaments are reorganized and polymerized for the enlargement of spine structure (Okamoto et al., 2004). Through what mechanism is structural plasticity performed? Because Tiam1 activates Rac1, its downstream molecules Pak and LIMK1 would also be activated, then LIMK1 phosphorylates Cofilin and inactivates its actin dissecting activity (Arber et al., 1998; Yang et al., 1998; Edwards, 1999). Because cofilin is a key molecule for actin turnover, the CaMKII-Tiam1-Rac1-Pak1-LIMK1-cofilin molecular pathway presumably modulates actin dynamics in dendritic spines. Other than this pathway, because the WAVE complex and the Arp2/3 complex work for actin bundling under Rac1, they might play a role in sLTP (Miki et al., 1998; Eden et al., 2002). Indeed, WAVE-1 Knock-out causes abnormal shapes of dendritic spines and Arp2/3 has an important role in the maintenance of spine structure (Soderling et al., 2007). Tiam1 works not only as a signaling molecule but also as a scaffolding molecule. Spinophilin binds to Tiam1 and this interaction regulates the actin cytoskeleton (Satoh et al., 1998; Buchsbaum et al., 2003). The role of WAVE-1 and Spinophilin is not yet understood on sLTP, but there is a possibility that the CaMKII signal includes these molecules and

anchors them to nearby stimulated spines.

The role of CaMKII-Tiam1-Rac1 signal for learning and memory

The necessity of NMDA receptors and CaMKII for LTP is known (Collingridge et al., 1983; Waxhamll, 1989; Malinow et al., 1989; Lynch et al., 2004). They are also required not only for sLTP but also learning and memory (Morris et al., 1986; McHugh et al., 1996; Silva et al., 1992). Are TIAM1 and Rac1 required for learning and memory? Tiam1 Knock-out mice are already reported but these reports did not focus on learning and memory. And there is no report on understanding the roles of Tiam1 for learning and memory (Malliri et al., 2002). However, Rac1 Knock-out showed a significant decrease of learning and memory scores in the Morris water maze (Haditsch et al., 2009). In our research, we reported that CaMKII-Tiam1 interaction is required for Rac1 activity, sLTP, and the maintenance of memory. PAK and WAVE-1 have important roles as well (Hayashi et al., 2004; Soderling et al., 2003). Interestingly, dominant-negative PAK transgenic mice showed an impairment of the memory consolidation process but not the memory acquirement process. This phenotype of PAK dominant-negative is similar to our Tiam1 mutation KI mice. And it suggests that the CaMKII-Tiam1-Rac1-PAK pathway is required for the maintenance of memory. On the other hand, the induction of sLTP causes the activation of RhoA and Cdc42, which are other Rho family small GTPases under NMDAR and CaMKII. In addition, Rac1-GEFs such as Karirin-7 and βPIX are also required for the structural change of dendritic spines. From these reports, CaMKII-Karirin-7/βPIX-Rac or CaMKII-unknown GEFs-RhoA/Cdc42 pathways might be required for other types of memory or other processes of memory e.g. memory acquirement or memory retrieval.

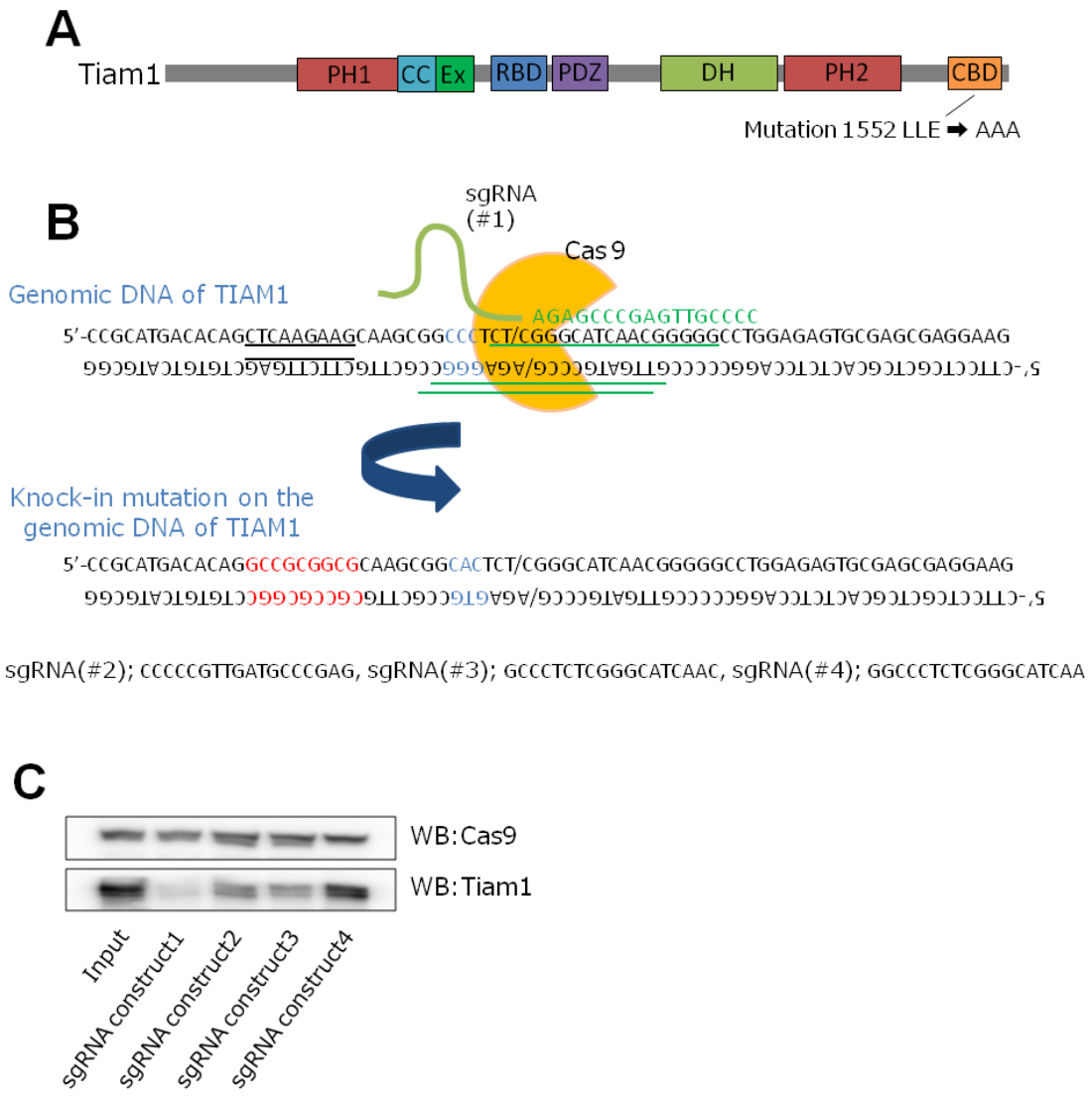

Figure 1. Design of sgRNAs mutation region on Tiam1 and the design of sgRNAs for genome editing.

A. Domain structure of Tiam1 and mutated region on CaMKII binding domain. PHn; N-terminal pleckstrin homology domain, CC-Ex; a coiled-coil region with adjacent sequence, RBD; Ras-binding domain, PDZ; PSD-95/DlgA/ZO-1 domain, DH; catalytic Dbl homology, PHc; C-terminal pleckstrin homology domain, CBD; CaMKII binding domain. **B**. Schematic demonstration of CRISPR/Cas9 mediated Knock-in mutation. The upper genomic DNA was double digested by Cas9 nuclease and guide

RNAs TIAM1(green sequence and under bars) on the CaMKII binding domain of TIAM1(under bars). The lower genomic DNA showed Knock-in mutation (red sequences) in the presence of homologous double strands oligo DNA. **C**. Immunoblot analysis to check several sgRNAs. TIAM1 was co-expressed with Cas9 and each sgRNA. The sgRNA#1 showed the most effective on-target effect.

B

Injection site	Number of eggs injected	Number of Successful duplications	Number of recipient mice	Successful Knock-in
Nucleus	200	139 (70 %)	13 (9 %)	3 hetero mice (23 %)
Cytoplasm	200	154 (77 %)	55 (36 %)	15 hetero and 4 homo mice (35 %)
Nucleus +Cytoplasm	100	41 (41 %)	1 (2 %)	1 hetero mouse (100 %)

Figure 2. Creation of TIAM1 mutant KI mice using CRISPR/Cas9 system.

A. Schematic diagram of generation of *tiam1* KI mice. **B**. Cas9 mRNA and sgRNA were injected into nucleus, cytoplasm or both of eggs after fertilization. As a result, 19 heterozygous and 4 homozygous *tiam1* KI mice were obtained. Injection into cytoplasm showed the highest survival rate and number of KI animals.

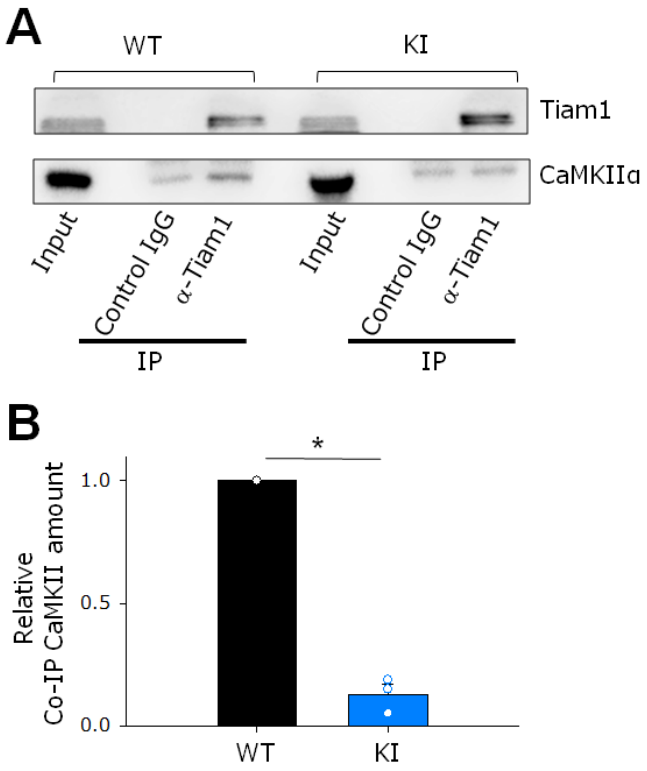

Figure 3. Lower amount of Co-IP CaMKII with TIAM1 in *tiam1* KI mice.

A. Co-Immunoprecipitation (Co-IP) of CaMKII with Tiam1 was performed using anti-Tiam1 antibody to check CaMKII-Tiam1 interaction. Upper bands indicate CaMKII and lower ones indicate Tiam1. Co-IP CaMKII with Tiam1 was observed compared to IgG control in WT mice. However, it could not be observed in KI mice. **B**. Quantitative analysis showed a significant decrease of Co-IP amount in KI mice. n= 3, from 9-11 week old mice, Student's *t*-test, *$p < 0.05$.

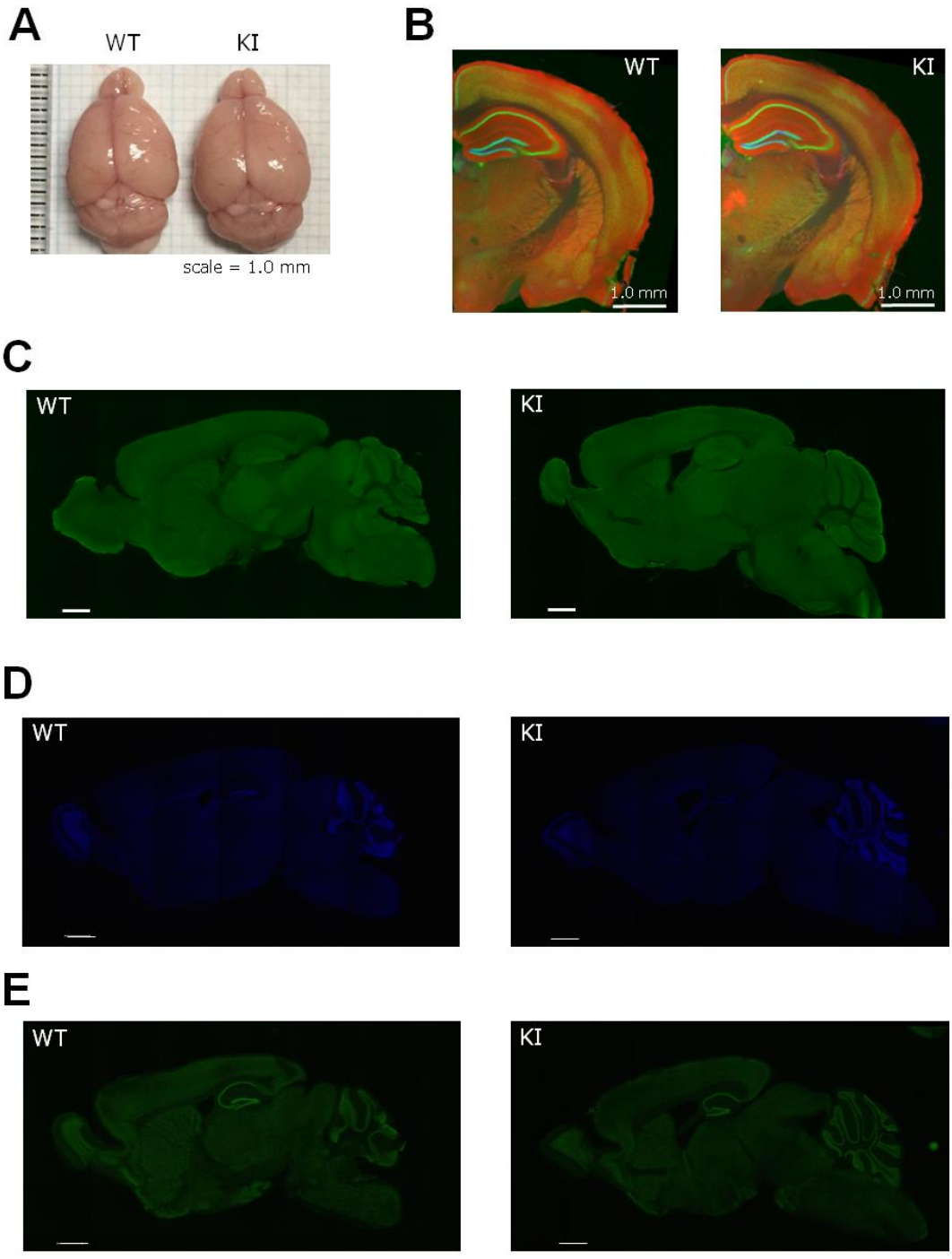
A
WT
KI
scale = 1.0 mm
B
WT
KI
1.0 mm
1.0 mm
C
WT
KI
D
WT
KI
E
WT
KI

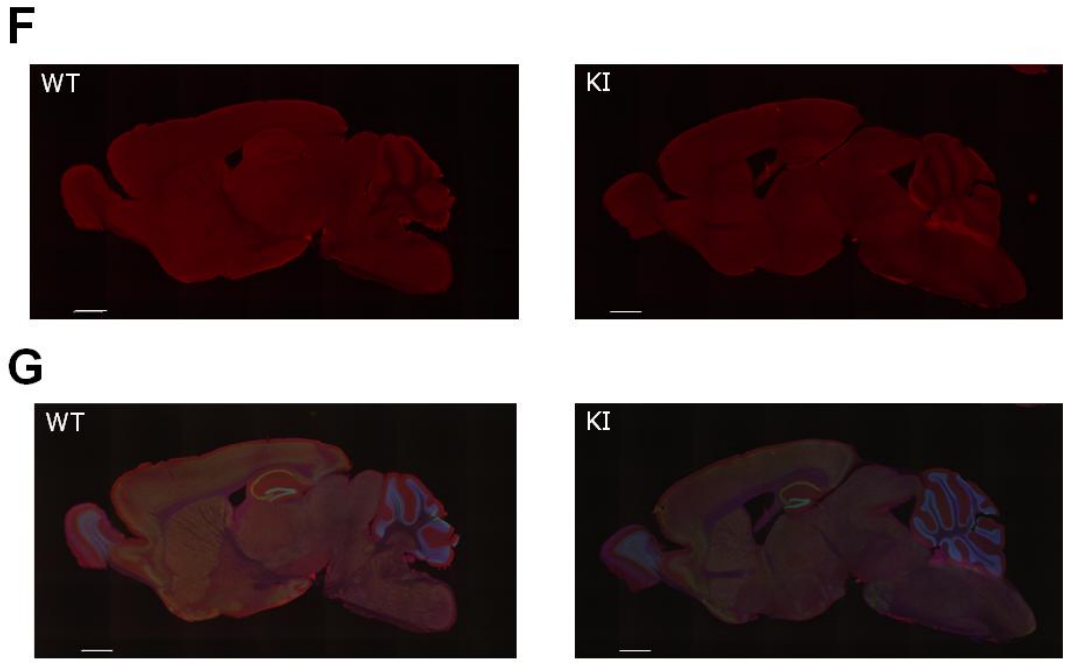

Figure 4. Whole brain structure in *tiam1* KI mice seemed to be same as in WT.

A. Pictures of whole brains from WT and KI mice. The brain size is not different between WT and KI mice. Scale bar 1 mm. **B**. Perfused coronal sections were stained by anti-NeuN antibody (green), Hoechst (blue), and Phalloidine (red). Scale bar 1 mm. **C**. Sagittal sections were stained with anti-Tiam1 antibody (green). **D**. Sagittal sections were stained with Hoechst (blue). **E**. Sagittal sections were stained with anti-NeuN antibody (green). **F**. Sagittal sections were stained with Phalloidine (red). **G**. Merge pictures from sagittal sections stained by anti-NeuN antibody (green), Hoechst (blue), and Phalloidine (red). Staining patterns and intensity of each signal were similar between WT and KI mice. Scale bar 1 mm. 10-11 week old mice.

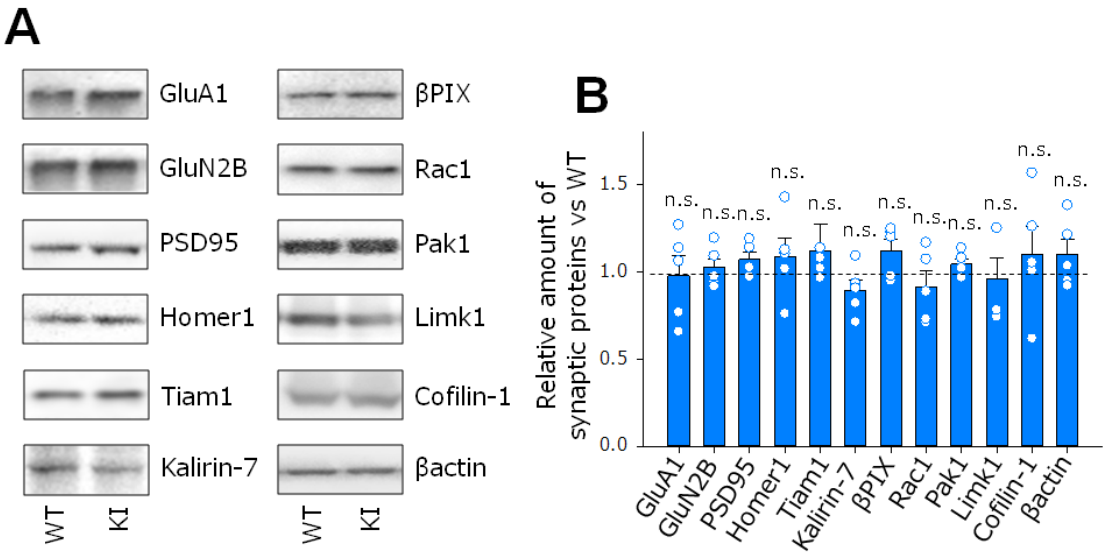

Figure 5. *tiam1* KI showed comparable expression of synaptic proteins to WT mice.

A. The immunoblot analysis showed a comparable expression of synaptic proteins in KI mice compared to WT mice. **B**. Quantitative analysis of each protein amount showed no significant difference between WT and KI mice. n= 5 each, from 9-11 week old mice, Student's *t*-test.

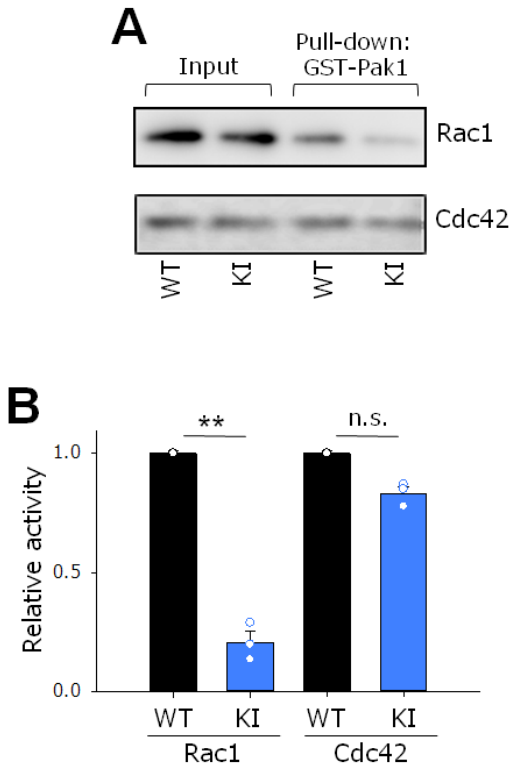

Figure 6. Rac activity is decreased in *tiam1* KI brain.

To measure Rac1 activity, pull-down assay with GST-PAK-CRIB (Cdc42 and Rac interactive binding domain) was performed. **A**. Upper bands indicate Rac1 and lower ones indicate Cdc42. The two lanes on the right hand show active proteins. **B**. The quantitative analysis of active Rac and Cdc42 amounts showed a specific reduction in Rac activity in KI mice compared to WT. However, the activity of Cdc42 in KI mice was comparable to WT. n=3 each, from 9-11 week old mice, Student's *t*-test, $^{**}p < 0.01$.

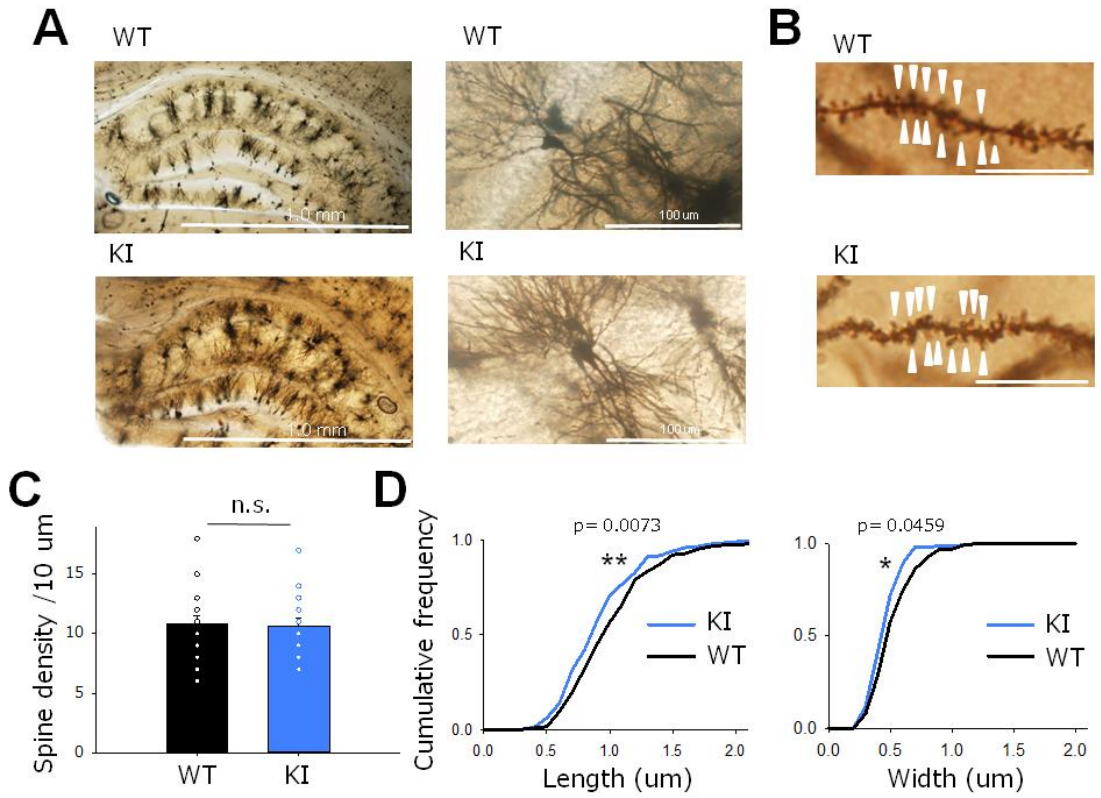

Figure 7. *tiam1* KI mice had short spine length and head width.

A. Representative Golgi-Cox staining images of hippocampus, CA1 pyramidal neurons from WT and KI mice brains. The structures of hippocampus and CA1 pyramidal neurons look similar between WT and KI mice. Scale bar 1 mm for the images of hippocampus. Scale bar 100 μm for the images of CA1 pyramidal neurons. **B**. Representative Golgi-Cox staining images of dendritic spines from WT and KI mice brains. Scale bar 10 μm. **C**. The quantitative analysis of spine numbers showed no significant difference between WT and KI mice. **D**. Cumulative curves showed a higher proportion of short-length and short head width of dendritic spines in KI mice compared to WT. n= 20 cells, from 9-11 week old male mice, Student's *t*-test, $^{**}p < 0.01$, $^{*}p < 0.05$.

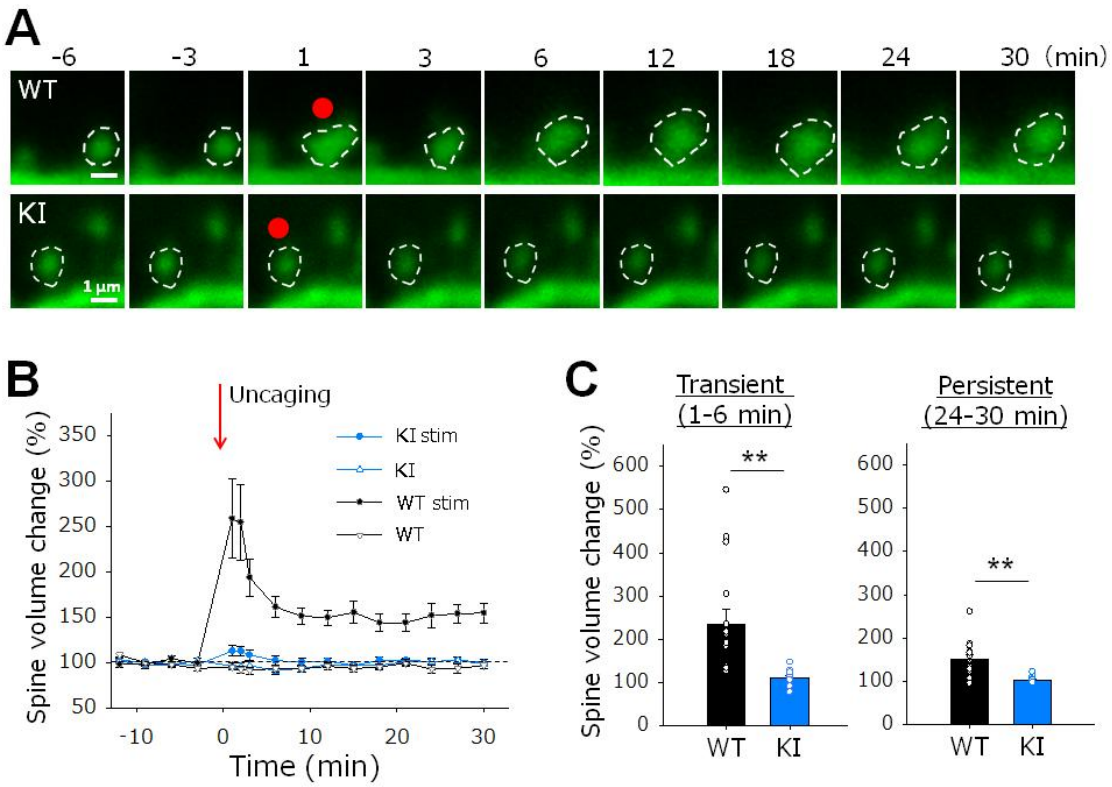

Figure 8. sLTP was impaired in *tiam1* KI mice.

A. Representative images of stimulated spines. The time at the top of each figure indicates the time from glutamate uncaging. Scale bar 1 μm. **B**. The traces indicate the volume change of each spine. The volume change of spines was observed in WT but not in KI mice. ●= stimulated spine, △= neighbor spine. **C**. The average volume change of spines in transient (1-3 min after stimulation) and sustained phase (21-30 min after stimulation) showed a significant decrease of volume enlargement after stimulation in KI mice. n=15 spines each from postnatal 7 day old pups, Student's t-test, **$p < 0.01$.

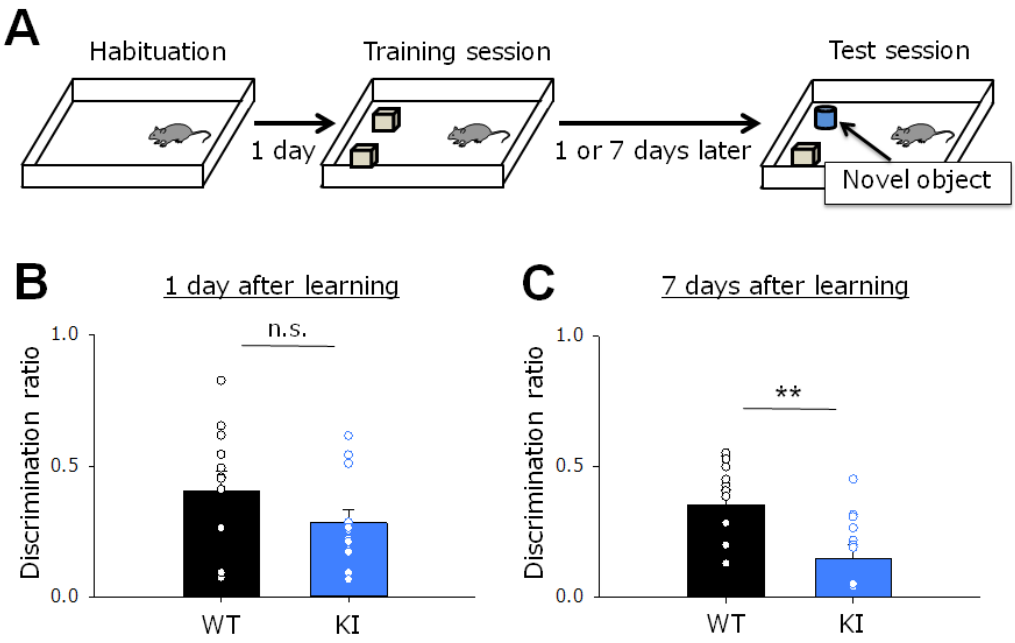

Figure 9. Long lasting memory was impaired in *tiam1* KI mice.

A. Behavioral paradigm of NORT. In the test session, one of the familiar objects which was used in the training session was replaced with a novel object. **B-C**. KI mice showed impaired memory 7 days after training. On day 1 after training, the significance was marginal. n= 12 each, Student's t-test, $^{**}p < 0.01$.

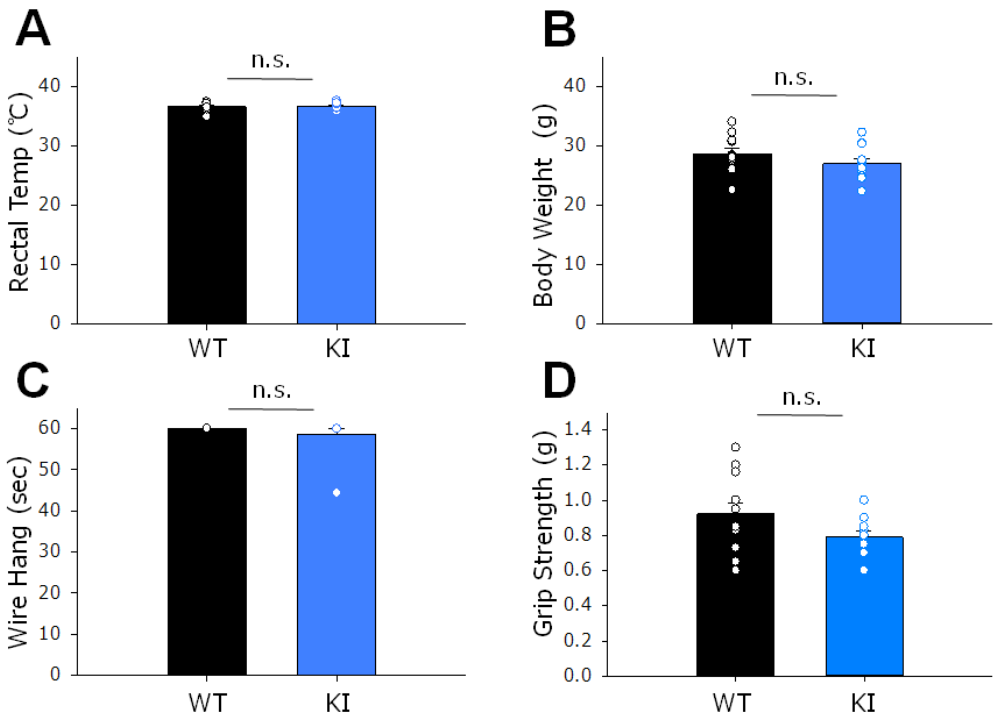

Figure 10. Rectal temperature, body weight and muscular strength were not different between WT and *tiam1* KI mice.

A. Rectal temperature was not significantly different between WT and KI mice. **B**. Body weight was not significantly different between WT and KI mice. **C**. To measure muscular strength, a wire hang test and a grip strength test were performed. In both tests, there were no significant differences of muscular strength. 8-14 week old male mice were used, n=12 for each, Student's t-test.

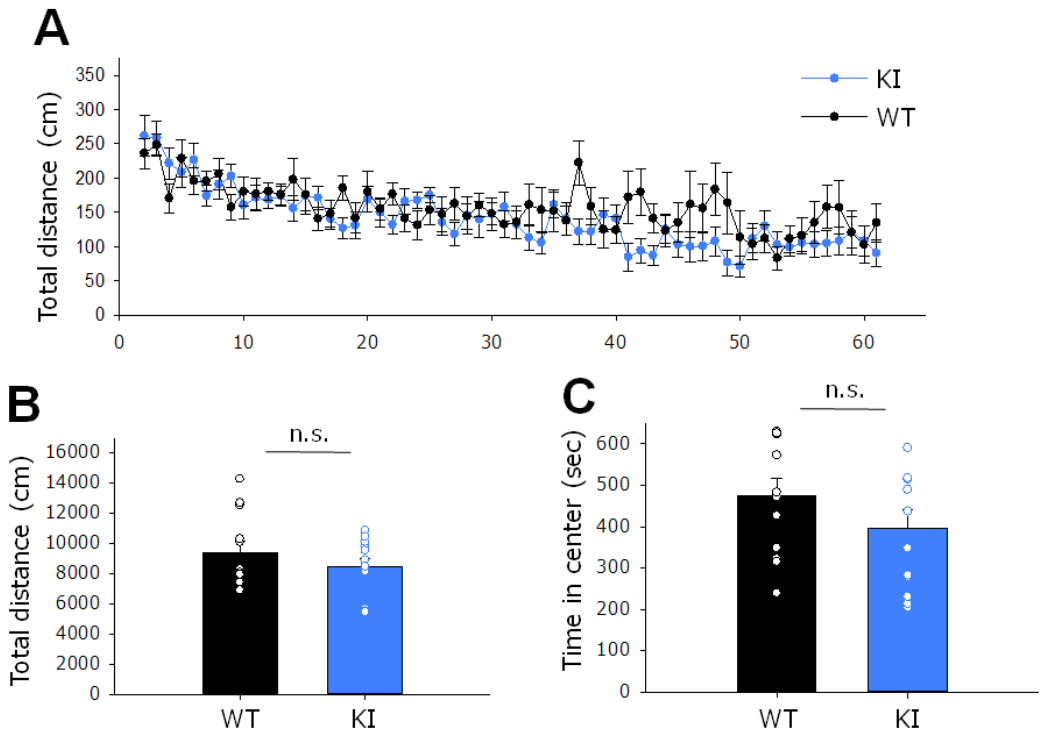

Figure 11. The open field test showed no difference between WT and *tiam1* KI mice.

A. The mice were allowed to move freely in the open field. The traces show the moved distance in every one minute. Both WT and KI mice showed a gradual decrease of the moved distance, which suggests, that both WT and KI mice got used to the environment. **B-C**. There was no difference of total distance in 1 hour and time spent in the center area of the open field (10 cm apart from the walls) between WT and KI mice. n=12 for each, Student's t-test. 8-14 week old male mice were used, n=12 each, one-way repeated ANOVA.

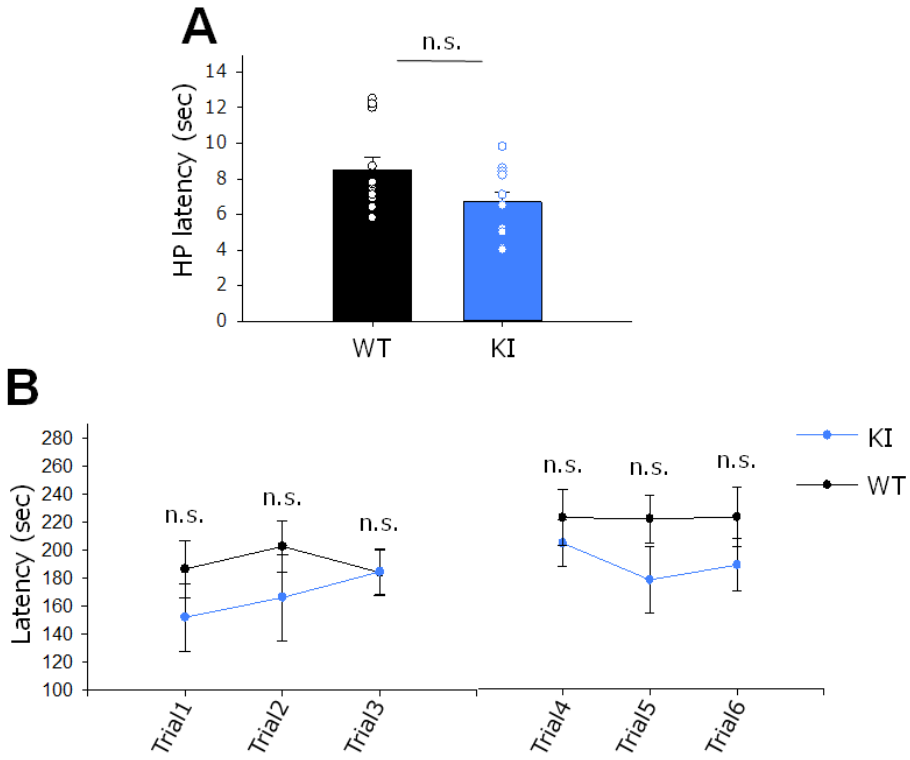

Figure 12. Normal thermal sensation and motor learning in *tiam1* KI mice.

A. The mice were placed on a hot plate at 55 °C and the time spent on the hot plate (sec) was measured as noxious thermal sensation. There was no difference of time spent between WT and KI mice. n=12 for each, Student's t-test. **B**. The mice were trained rotarod 3 times per day. The latency to fall down from the rotor rod was measured as motor learning. There is no significant difference of the latency between WT and KI mice. 8-14 weeks old male mice were used, n=12 each, Bonferoni test after one-way repeated ANOVA.

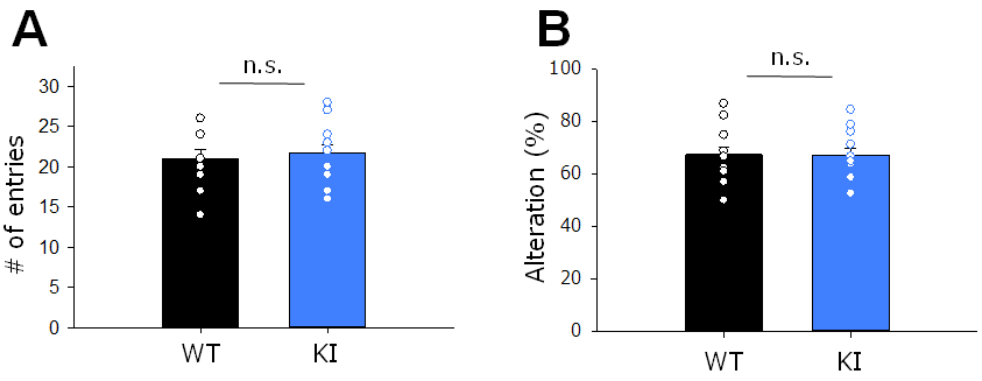

Figure 13. Normal working memory and no schizophrenia-like behavior in *tiam1* KI mice.

A-B. The mice were allowed to freely move for 5 min in a Y-maze and the number of entries into an arm as well as the total alteration were measured as working memory and schizophrenia-like behavior. There were no differences in the number of entries into arm or total alteration between WT and KI mice. 8-14 week old male mice were used, n=12 each, Student's t-test.

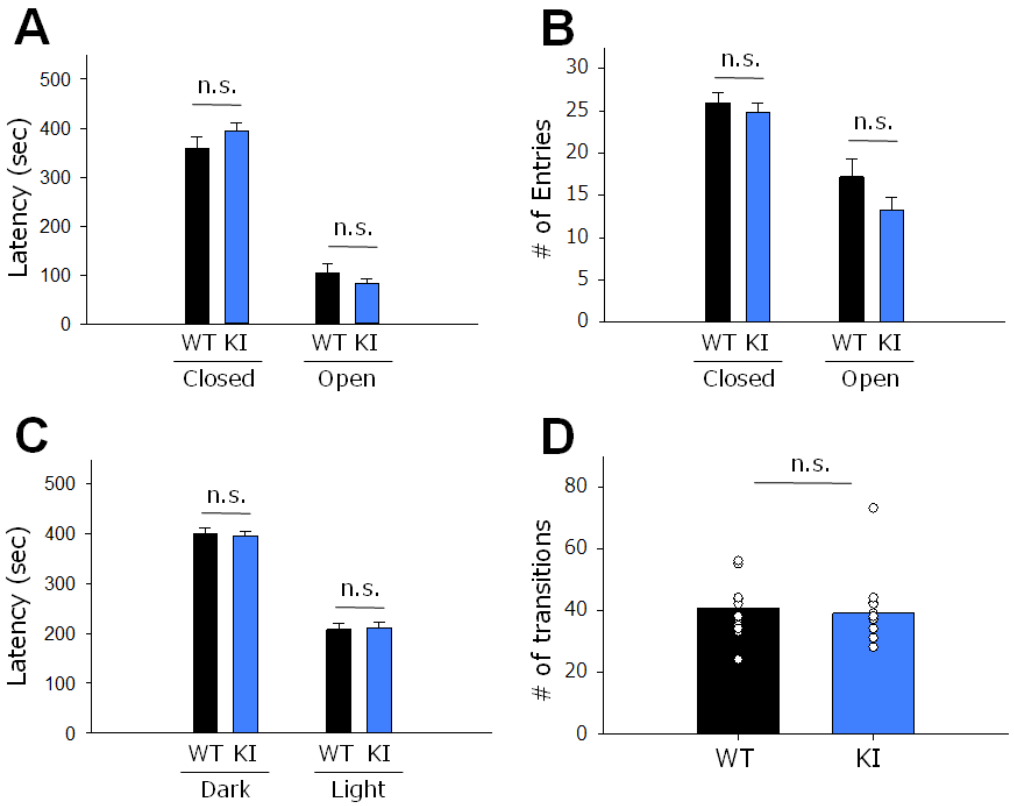

Figure 14. No anxiety-like behavior in *tiam1* KI mice.

A-B. The mice were allowed to move on an elevated plus maze. The latency in each arm and the number of entries into each arm were measured. There was no increase of latency in the closed arms or the number of entries into the closed arms as anxiety-like behaviors in KI mice. **C-D**. The mice were allowed to move in a light/dark transition maze and the latency in each room as well as the number of transitions between light and dark room were measured. There was no increase of latency in the dark room or the number of transitions into the dark room as anxiety-like behavior in KI mice. 8-14 week old male mice were used, n=12 for each, Student's t-test.

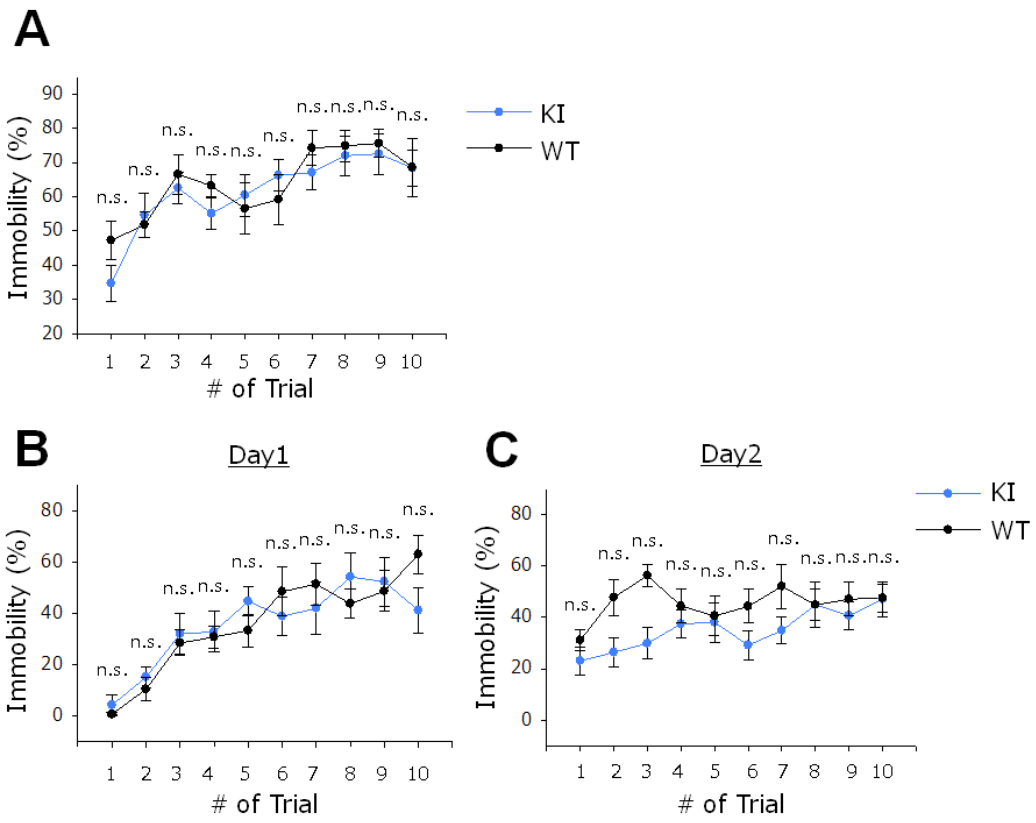

Figure 15. No depression-like behavior in *tiam1* KI mice.

A. Result of Porsolt forced swim test. The mice were forced to swim in a plastic cylinder filled with water for 10 min and immobile time within every 1 min was measured as a depression-like behavior. There was no difference of immobile time between WT and KI mice. **B-C**. Tail suspension test. The mice were suspended from 30 cm above the floor for 10 min per day, for two days and immobile time within every 1 min was measured as a depression-like behavior. There was no difference of immobile time between WT and KI mice. 8-14 week old male mice were used. n=12 each, Bonferoni test after one-way repeated ANOVA.

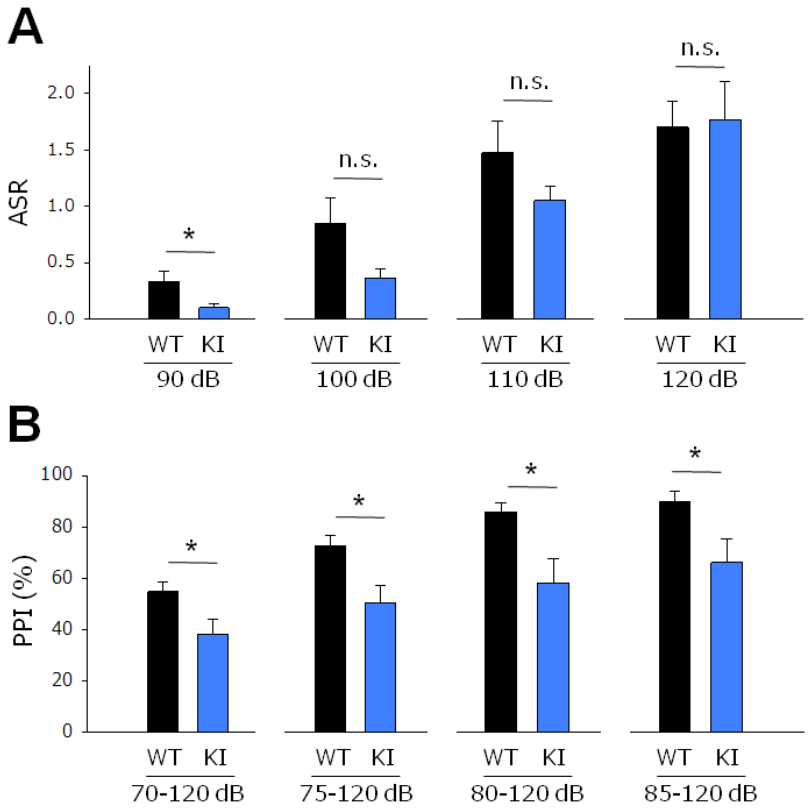

Fig 16. Prepulse inhibition was reduced in KI mice.

A. The startle response to 90, 100, 110 or 120 dB stimuli was measured. Acoustic startle response (ASR) was defined according to the largest peak-to-peak voltage deflection from startle movements. There was no significant difference between WT and KI. **B**. A prepulse inhibition test was performed as a schizophrenia-like behavior. The KI mice showed a significant decrease of prepulse inhibition as compared to WT for each combination of prepulse and startle stimuli (70–120, 75–120, 80–120, and 85–120 dB). This result suggests, that KI mice have a schizophrenia-like phenotype. 8-14 week old male mice were used. n=12 each, Student's *t*-test, *$p < 0.05$.

References

Arber, S., Barbayannis, F. A., Hanser, H., Schneider, C., Stanyon, C. A., Bernard, O., & Caroni, P. (1998). Regulation of actin dynamics through phosphorylation of cofilin by LIM-kinase. *Nature*, *393*(6687), 805-809.

Bosch, M., Castro, J., Saneyoshi, T., Matsuno, H., Sur, M., & Hayashi, Y. (2014). Structural and molecular remodeling of dendritic spine substructures during long-term potentiation. *Neuron*, *82*(2), 444-459.

Buchsbaum, R. J., Connolly, B. A., & Feig, L. A. (2003). Regulation of p70 S6 kinase by complex formation between the Rac guanine nucleotide exchange factor (Rac-GEF) Tiam1 and the scaffold spinophilin. *Journal of Biological Chemistry*, *278*(21), 18833-18841.

Collingridge, G. L., Kehl, S. J., & McLennan, H. T. (1983). Excitatory amino acids in synaptic transmission in the Schaffer collateral-commissural pathway of the rat hippocampus. *The Journal of physiology*, *334*(1), 33-46.

Cong, L., Ran, F. A., Cox, D., Lin, S., Barretto, R., Habib, N., ... & Zhang, F. (2013). Multiplex genome engineering using CRISPR/Cas systems. *Science*, 1231143.

Edwards, D. C. (1999). Activation of LIM-kinase by Pak1 couples Rac/Cdc42 GTPase signaling to actin cytoskeletal dynamics. *Nat. Cell Biol.*, *1*, 115.

Erondu, N. E., & Kennedy, M. B. (1985). Regional distribution of type II Ca2+/calmodulin-dependent protein kinase in rat brain. *Journal of Neuroscience*, *5*(12), 3270-3277.

Fleming, I. N., Elliott, C. M., Buchanan, F. G., Downes, C. P., & Exton, J. H. (1999). Ca2+/calmodulin-dependent protein kinase II regulates Tiam1 by reversible protein phosphorylation. *Journal of Biological Chemistry*, *274*(18), 12753-12758.

Geyer, M. A., Krebs-Thomson, K., Braff, D. L., & Swerdlow, N. R. (2001). Pharmacological studies of prepulse inhibition models of sensorimotor gating deficits in schizophrenia: a decade in review. *Psychopharmacology*, *156*(2-3), 117-154.

Haditsch, U., Leone, D. P., Farinelli, M., Chrostek-Grashoff, A., Brakebusch, C., Mansuy, I. M., ... & Palmer, T. D. (2009). A central role for the small GTPase Rac1 in hippocampal plasticity and spatial learning and memory. *Molecular and Cellular Neuroscience*, *41*(4), 409-419.

Hayashi, M. L., Choi, S. Y., Rao, B. S., Jung, H. Y., Lee, H. K., Zhang, D., ... & Tonegawa, S. (2004). Altered cortical synaptic morphology and impaired memory consolidation in forebrain-specific dominant-negative PAK transgenic mice. *Neuron*, *42*(5), 773-787.

Hedrick, N. G., Harward, S. C., Hall, C. E., Murakoshi, H., McNamara, J. O., & Yasuda, R. (2016). Rho GTPase complementation underlies BDNF-dependent homo-and heterosynaptic plasticity. *Nature*, *538*(7623), 104.

Kang, H. W., Kim, H. K., Moon, B. H., Lee, S. J., & Lee, S. J. (2017). Comprehensive Review of Golgi Staining Methods for Nervous Tissue. *Applied Microscopy*, *47*(2), 63-69.

Kim, K., Lakhanpal, G., Lu, H. E., Khan, M., Suzuki, A., Hayashi, M. K., ... & Blanpied, T. A. (2015). A temporary gating of actin remodeling during synaptic plasticity consists of the interplay between the kinase and structural functions of CaMKII. *Neuron*, *87*(4), 813-826.

Lee, S. J. R., Escobedo-Lozoya, Y., Szatmari, E. M., & Yasuda, R. (2009). Activation of CaMKII in single dendritic spines during long-term potentiation. *Nature*, *458*(7236), 299.

Lu, W. Y., Man, H. Y., Ju, W., Trimble, W. S., MacDonald, J. F., & Wang, Y. T. (2001). Activation of synaptic NMDA receptors induces membrane insertion of new AMPA receptors and LTP in cultured hippocampal neurons. *Neuron*, *29*(1), 243-254.

Lynch, M. A. (2004). Long-term potentiation and memory. *Physiological reviews*, *84*(1), 87-136.

Malinow, R., Schulman, H., & Tsien, R. W. (1989). Inhibition of postsynaptic PKC or

CaMKII blocks induction but not expression of LTP. *Science*, *245*(4920), 862-866.

Matsuzaki, M., Honkura, N., Ellis-Davies, G. C., & Kasai, H. (2004). Structural basis of long-term potentiation in single dendritic spines. *Nature*, *429*(6993), 761-766.

McHugh, T. J., Blum, K. I., Tsien, J. Z., Tonegawa, S., & Wilson, M. A. (1996). Impaired hippocampal representation of space in CA1-specific NMDAR1 knockout mice. *Cell*, *87*(7), 1339-1349.

Miki, H., Suetsugu, S., & Takenawa, T. (1998). WAVE, a novel WASP-family protein involved in actin reorganization induced by Rac. *The EMBO journal*, *17*(23), 6932-6941

Morris, R. G. M., Anderson, E., Lynch, G. A., & Baudry, M. (1986). Selective impairment of learning and blockade of long-term potentiation by an N-methyl-D-aspartate receptor antagonist, AP5. *Nature*, 319(6056), 774.

Nabavi, S., Fox, R., Proulx, C. D., Lin, J. Y., Tsien, R. Y., & Malinow, R. (2014). Engineering a memory with LTD and LTP. *Nature*, *511*(7509), 348.

O'Callaghan, J. P., & Holtzman, S. G. (1975). Quantification of the analgesic activity of narcotic antagonists by a modified hot-plate procedure. *Journal of Pharmacology and Experimental Therapeutics*, *192*(3), 497-505.

Okamoto, K. I., Nagai, T., Miyawaki, A., & Hayashi, Y. (2004). Rapid and persistent modulation of actin dynamics regulates postsynaptic reorganization underlying bidirectional plasticity. *Nature neuroscience*, *7*(10), 1104-1112.

Okamoto, K. I., Narayanan, R., Lee, S. H., Murata, K., & Hayashi, Y. (2007). The role of CaMKII as an F-actin-bundling protein crucial for maintenance of dendritic spine structure. *Proceedings of the National Academy of Sciences*, *104*(15), 6418-6423.

Satoh, A., Nakanishi, H., Obaishi, H., Wada, M., Takahashi, K., Satoh, K., ... & Takai, Y. (1998). Neurabin-II/spinophilin an actin filament-binding protein with one pdz domain localized at cadherin-based cell-cell adhesion sites. *Journal of Biological*

Chemistry, *273*(6), 3470-3475.

Saneyoshi, T., Wayman, G., Fortin, D., Davare, M., Hoshi, N., Nozaki, N., ... & Soderling, T. R. (2008). Activity-dependent synaptogenesis: regulation by a CaM-kinase kinase/CaM-kinase I/βPIX signaling complex. *Neuron*, *57*(1), 94-107.

Shan, Q., Wang, Y., Li, J., & Gao, C. (2014). Genome editing in rice and wheat using the CRISPR/Cas system. *Nature protocols*, *9*(10), 2395.

Silva, A. J., Paylor, R., Wehner, J. M., & Tonegawa, S. (1992). Impaired spatial learning in alpha-calcium-calmodulin kinase II mutant mice. *Science*, *257*(5067), 206-211.

Silva, A. J., Stevens, C. F., Tonegawa, S., & Wang, Y. (1992). Deficient hippocampal long-term potentiation in alpha-calcium-calmodulin kinase II mutant mice. *Science*, *257*(5067), 201-206.

Soderling, S. H., Guire, E. S., Kaech, S., White, J., Zhang, F., Schutz, K., ... & Scott, J. D. (2007). A WAVE-1 and WRP signaling complex regulates spine density, synaptic plasticity, and memory. *The Journal of neuroscience*, *27*(2), 355-365.

Soderling, S. H., Langeberg, L. K., Soderling, J. A., Davee, S. M., Simerly, R., Raber, J., & Scott, J. D. (2003). Loss of WAVE-1 causes sensorimotor retardation and reduced learning and memory in mice. *Proceedings of the National Academy of Sciences*, *100*(4), 1723-1728.

Tolias, K. F., Bikoff, J. B., Burette, A., Paradis, S., Harrar, D., Tavazoie, S., ... & Greenberg, M. E. (2005). The Rac1-GEF Tiam1 couples the NMDA receptor to the activity-dependent development of dendritic arbors and spines. *Neuron*, *45*(4), 525-538.

Tolias, K. F., Bikoff, J. B., Kane, C. G., Tolias, C. S., Hu, L., & Greenberg, M. E. (2007). The Rac1 guanine nucleotide exchange factor Tiam1 mediates EphB receptor-dependent dendritic spine development. *Proceedings of the National Academy of Sciences*, *104*(17), 7265-7270.

Tsien, J. Z., Huerta, P. T., & Tonegawa, S. (1996). The essential role of hippocampal CA1 NMDA receptor–dependent synaptic plasticity in spatial memory. *Cell*, *87*(7), 1327-1338.

Tsui, J., Inagaki, M., & Schulman, H. (2005). Calcium/calmodulin-dependent protein kinase II (CaMKII) localization acts in concert with substrate targeting to create spatial restriction for phosphorylation. *Journal of Biological Chemistry*, *280*(10), 9210-9216.

Waxhamll, N. N. (1989). An essential role for postsynaptic calmodulin and protein kinase activity in long-term potentiation. *Nature* , *340*(6234), 554.

Whitlock, J. R., Heynen, A. J., Shuler, M. G., & Bear, M. F. (2006). Learning induces long-term potentiation in the hippocampus. *Science*, *313*(5790), 1093-1097.

Worthylake, D. K., Rossman, K. L., & Sondek, J. (2000). Crystal structure of Rac1 in complex with the guanine nucleotide exchange region of Tiam1. *Nature*, *408*(6813), 682.

Xu, W., & Südhof, T. C. (2013). A neural circuit for memory specificity and generalization. *Science*, *339*(6125), 1290-1295.

Yamasaki, N., Maekawa, M., Kobayashi, K., Kajii, Y., Maeda, J., Soma, M., ... & Kanzaki, K. (2008). Alpha-CaMKII deficiency causes immature dentate gyrus, a novel candidate endophenotype of psychiatric disorders. *Molecular brain*, *1*(1), 6.

Yang, N., Higuchi, O., Ohashi, K., Nagata, K., Wada, A., Kangawa, K., ... & Mizuno, K. (1998). Cofilin phosphorylation by LIM-kinase 1 and its role in Rac-mediated actin reorganization. *Nature*, *393*(6687), 809-812.

Zhang, H., & Macara, I. G. (2006). The polarity protein PAR-3 and TIAM1 cooperate in dendritic spine morphogenesis. *Nature cell biology*, *8*(3), 227.

Zaqout, S., & Kaindl, A. M. (2016). Golgi-cox staining step by step. *Frontiers in*

neuroanatomy, *10*, 38.

Acknowledgements

My research was performed with a lot of support and help from The University of Tokyo, RIKEN Center for Brain Science and Kyoto University.
I especially want to thank the Support Unit for Animal Resources Development in RIKEN for generating the tiam1 KI mice and the Behavior Facility in Kyoto University for conducting the behavioral battery test.

In addition, I am deeply grateful for the financial support from the Graduate Program for Leaders in Life Innovation (GPLLI). The GPLLI program gave me the opportunity to take part in lecture courses from professors of different graduate courses, work in a laboratory of choice of a different graduate course, as well as taking part in workshops and study abroad. I received many stimuli from a lot of people with different backgrounds through this experience.

Furthermore, I owe my deep gratitude to Prof. Yuji Ikegaya for giving me the opportunity to study in different laboratories, educating me and giving cheerful comments when I was really depressed and tried to quit the graduate course. I respect him not only as a professional scientist but also as a great educator. The things I learnt from him will definitely be helpful for me also in the future.

I would also like to express my appreciation to Dr. Ryuta Koyama. I could learn from his way of thinking and positive attitude towards science, as well as his research style. His kind comments also cheered me up.

Moreover, I am grateful to Dr. Hiroshi Nomura as my first supervisor. I learnt not only experimental skills from him but also a way of thinking and attitude towards research.

I also want to thank Dr. Takuya Sasaki. His way of thinking in scientific discussions is very logical and it was an inspiration for me.

Likewise, I would like to express my appreciation to Ai Nakashima and Haruki Takeuchi. Because their research is comparably similar to my research, their comments have been very helpful in advancing in my research.

In terms of teaching me basic skills for research and a lot of knowledge as well as

giving me advice for life, I would like to thank Natsuko Hitora, Sakiko Toyoda, Kenta Funayama, Daisuke Nakayama, Chiaki Kobayashi, Hiroaki Norimoto, Nobuyoshi Matsumoto, Yuuki Miura, Tetsuya Sakaguchi, Kazuki Shibata, Hikaru Igarashi, Tomoe Ishikawa, Koshiro Hara, Takeyuki Miyawaki, Kosuke Onoue, Atsuko Kobayashi, Tomoya Kitagawa and Chie Teshirogi.

As my colleagues in the laboratory of Chemical Pharmacology, I am indebted to Kenichi Makino, Zhiwen Zhou, Satoshi Iwasaki, Kazuki Okamoto, Mami Okada, Yu Shikano, Kohei Morishita, Hideki Ueda, Nariaki Uemura. They have great ability and passion for research. Because I had great colleagues like them, I could continue the doctoral course.

Furthermore, I would like to thank all members in the Laboratory of Chemical Pharmacology of the University of Tokyo.

In addition, I am deeply thankful to Prof. Yasunori Hayashi in Kyoto University for giving me the opportunity to study in his laboratory and teaching me many things about science. I have greatly benefitted from his always kind teaching of research skills and knowledge. I respect him from the bottom of my heart.

Moreover, I would like to thank Dr. Takeo Saneyoshi in Kyoto University for teaching me research skills and knowledge especially for the molecular biology part. His supervision was always helpful to overcome difficulties and my research was inspired by his research.

Finally, I want to thank my family: Takayuki Kojima, Masako Kojima, Naoto Kojima, Yuto Kojima, Mitsue Kojima and my fiancée Manuela Küng for supporting me. Their mental, physical and financial support are the base of my life.